

# Finding Defective Elements in Intelligent Reflecting Surface via Over-the-Air Measurements

Ziyi Zhao\*, Zhaorui Wang<sup>†</sup>, Shuowen Zhang\*, and Liang Liu\*

\*Department of Electrical and Electronic Engineering, The Hong Kong Polytechnic University, Hong Kong SAR, China,

E-mail: ziyi.zhao@connect.polyu.hk, {shuowen.zhang,liang-eie.liu}@polyu.edu.hk

<sup>†</sup>School of Science and Engineering, The Chinese University of Hong Kong, Shenzhen, Shenzhen, China

E-mail: wangzhaorui@cuhk.edu.cn

**Abstract**—Due to circuit failures, defective elements that cannot adaptively adjust the phase shifts of their impinging signals in a desired manner may exist on an intelligent reflecting surface (IRS). Traditional way to find these defective IRS elements requires a thorough diagnosis of all the circuits belonging to a huge number of IRS elements, which is practically challenging. In this paper, we will devise a novel approach under which a transmitter sends known pilot signals and a receiver localizes all the defective IRS elements just based on its over-the-air measurements reflected from the IRS. The key lies in the fact that the over-the-air measurements at the receiver side are functions of the set of defective IRS elements. Based on this observation, we propose a bisection based method to localize all the defective IRS elements. Specifically, at each time slot, we properly control the desired phase shifts of all the IRS elements such that half of the considered regime that is not useful to localize the defective elements can be found based on the received signals and removed. Via numerical results, it is shown that our proposed bisection method can exploit the over-the-air measurements to localize all the defective IRS elements quickly and accurately.

## I. INTRODUCTION

The recent revolution in software-controlled surfaces using metamaterials has stimulated a flurry of research activities in using intelligent reflecting surface (IRS) to improve the performance for wireless communication [1]–[4]. The key is to adaptively adjust the phase shifts of IRS elements based on the channel state information (CSI) so as to enhance the channel quality of the mobile users. Previously, tremendous works have been done to enable low-overhead CSI acquisition [5]–[8] and efficient IRS phase shift design based on CSI [9]–[13], assuming that all IRS elements are in the normal state and able to induce the desired phase shifts via properly controlling their circuits. However, in practice, the circuits of IRS elements are prone to failures [14]. Therefore, it is very likely that some defective elements that cannot adaptively achieve the desired reflecting patterns exist on the IRS. For example, if there is a circuit failure in a controller chip such that it cannot consistently send the desired phase shifts to its associated IRS elements, the phase shifts of these defective elements will be

stuck at a fixed state. This motivates us to study the diagnosis of the IRS in this paper.

A conventional approach for a diagnosis of the IRS is to have a thorough check of all its circuits. However, this approach is practically challenging, because there are a huge number of sophisticated circuits to control hundreds of or even thousands of IRS elements. In this paper, we propose a novel approach that is able to find all the defective IRS elements just based on the over-the-air measurements. To enable an over-the-air diagnosis of the IRS, a transmitter and a receiver are deployed around the IRS. Under this system, the transmitter keeps transmitting known pilot signals, the IRS elements keep changing their phase shifts in a pre-designed pattern, and the receiver measures its received signals. Because of the defective IRS elements, the received signals can be quite different from the expected ones. The key observation is that the abnormal received signals are functions of the set of the defective IRS elements. This motivates us to apply the bisection method to estimate this set based on the received signals. Specifically, an efficient way to adaptively control the desired phase shifts of all the IRS elements is designed such that we are able to iteratively find a sub-regime on the IRS that is not useful to localize the defective IRS elements. After iteratively removing these sub-regimes based on the bisection method, we can localize all the defective IRS elements. Because the bisection method can cut off half of the remaining regime at each iteration, our proposed method is very efficient to localize the defective elements from a huge number of IRS elements.

It is worth noting that a related topic, hardware impairment, has been investigated in the literature [15]–[18]. In these works, it is assumed that an unknown phase error is added to the desired phase shift of each IRS element. Based on this model, various signal processing techniques have been proposed to estimate these phase errors such that calibration can be conducted to compensate for these phase errors. However, circuit failure considered in this paper is quite different from hardware impairment considered in the above works. Specifically, under the hardware impairment model, the phase shifts of all IRS elements are still close to the desired values, just subject to some errors. However, under the circuit failure model, some IRS elements are totally in the irregular state, and the phase

The work was supported in part by the National Key R&D Project of China under Grant No. 2022YFB2902800; by the National Natural Science Foundation of China with Grant No. 62101474; and by the Research Grants Council, Hong Kong, China, with Grant No. 15203222 and Grant No. 15230022.

shifts of these defective elements usually have nothing to do with the desired values, e.g., they are stuck at fixed values. Due to this reason, calibration is not possible under our considered model. We have to localize all the defective IRS elements, even though we do not know their irregular reflecting patterns, such that we can repair their circuits. This is a new problem.

## II. SYSTEM MODEL

Consider an IRS consisting of  $N = N_h \times N_v$  elements, which are laid out in a grid pattern with  $N_h$  columns and  $N_v$  rows. Without loss of generality, we assume that  $N_h = 2^{m_h}$  and  $N_v = 2^{m_v}$  with some integers  $m_h$  and  $m_v$ . Define  $\mathcal{N}_h = \{1, \dots, N_h\}$  and  $\mathcal{N}_v = \{1, \dots, N_v\}$ . Moreover, we index the element at the  $n_h$ -th column and the  $n_v$ -th row of the IRS as element  $(n_h, n_v)$ ,  $n_h \in \mathcal{N}_h$ ,  $n_v \in \mathcal{N}_v$ .

Because of the complicated circuit to control the reflecting patterns, the elements on an IRS are prone to failures. The defective IRS elements may not reflect the signals in the pre-designed pattern, leading to poor communication performance. If an IRS is in an irregular state with some defective elements, our objective is to find the indices of all the defective elements.

### A. IRS Failure Model

In this paper, we consider a clustered failure model of the IRS [14], where all the defective elements are located within a continuous rectangular region of the IRS,<sup>1</sup> as shown in Fig. 1. Such a model is valid in many scenarios, e.g., when a controller chip fails to send control signals to its associated elements, when faults in some interconnects leave a clustered region of the IRS isolated from the remaining region, etc. Let  $(n_{h,\min}, n_{v,\min})$  and  $(n_{h,\max}, n_{v,\max})$  denote the indices of the elements at the lower left corner and the upper right corner of this defective region, respectively, as shown in Fig. 1. Therefore, under our considered clustered failure model, the set consisting of the indices of all the defective elements on the IRS is given by

$$\mathcal{E} = \{(n_h, n_v) | n_h \in \{n_{h,\min}, \dots, n_{h,\max}\}, n_v \in \{n_{v,\min}, \dots, n_{v,\max}\}\}. \quad (1)$$

For simplicity, we also define the set consisting of the indices of all the IRS elements in the normal state as

$$\mathcal{W} = \{(n_h, n_v) | (n_h, n_v) \notin \mathcal{E}\}. \quad (2)$$

Let  $\phi_{n_h, n_v, t} \in (0, 2\pi]$  and  $e^{j\phi_{n_h, n_v, t}}$  denote the desired phase shift and the corresponding reflecting coefficient of IRS element  $(n_h, n_v)$  at time slot  $t$ ,  $\forall n_h \in \mathcal{N}_h$ ,  $n_v \in \mathcal{N}_v$ . For each IRS element  $(n_h, n_v) \in \mathcal{W}$  that is in the normal state, it will adaptively reflect the signals with different phase shifts at different time slots. However, for any defective IRS element  $(n_h, n_v) \in \mathcal{E}$ , we assume that it is stuck at a constant

<sup>1</sup>If the defective elements are located within a continuous but non-rectangular region of the IRS, the defective element set  $\mathcal{E}$  defined in (1) actually is the minimum rectangular region that contains all the defective elements. After such a small region is found based on the over-the-air approach that is later proposed in the paper, we can have a quick diagnosis of circuits of all the elements in  $\mathcal{E}$  to further localize the defective elements.

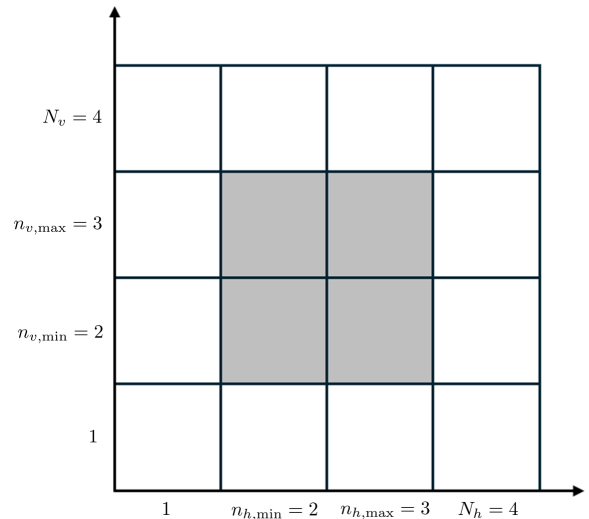


Fig. 1. An IRS with clustered defective IRS elements (in gray): there are  $N_v = 4$  rows and  $N_h = 4$  columns of elements on the IRS, and the indices of the defective elements are  $(2, 2)$ ,  $(2, 3)$ ,  $(3, 2)$ , and  $(3, 3)$ .

but unknown state over different time slots [14]. This can occur when a controller chip fails to send control signals to its associated elements, such that these elements cannot adaptively update their reflecting coefficients as desired. Under this error pattern, the constant phase shift and the corresponding reflecting coefficient of a defective element  $(n_h, n_v) \in \mathcal{E}$  across all the time slots are defined as  $\beta_{n_h, n_v} \in (0, 2\pi]$  and  $e^{j\beta_{n_h, n_v}}$ , respectively. In practice, the real reflecting coefficient of IRS element  $(n_h, n_v)$  at time slot  $t$ , which depends on whether this element is defective or not, is given by

$$\theta_{n_h, n_v, t} = \begin{cases} e^{j\phi_{n_h, n_v, t}}, & \text{if } (n_h, n_v) \in \mathcal{W}, \\ e^{j\beta_{n_h, n_v}}, & \text{if } (n_h, n_v) \in \mathcal{E}, \end{cases} \quad \forall t. \quad (3)$$

Note that under the above reflecting model,  $\beta_{n_h, n_v}$  and  $\mathcal{E}$  (also  $\mathcal{W}$ ) are unknown. Therefore,  $\theta_{n_h, n_v, t}$  is also unknown.

### B. Signal Model

In this paper, we aim to propose an over-the-air approach to estimate the values of  $n_{h,\min}$ ,  $n_{h,\max}$ ,  $n_{v,\min}$ , and  $n_{v,\max}$  such that we can find the indices of all the defective elements on the IRS, i.e.,  $\mathcal{E}$ . To enable the over-the-air diagnosis of the IRS, we deploy a radio transmitter and a radio receiver around the IRS. It is assumed that the transmitter is equipped with 1 antenna, while the receiver is equipped with  $M \geq 1$  antennas. Define  $\mathbf{h} \in \mathbb{C}^{M \times 1}$  as the channel from the transmitter to the receiver,  $\mathbf{u}_{n_h, n_v}$  as the channel from the transmitter to IRS element  $(n_h, n_v)$ , and  $\mathbf{r}_{n_h, n_v} \in \mathbb{C}^{M \times 1}$  as the channel from IRS element  $(n_h, n_v)$  to the receiver. We assume that the transmitter and the receiver are deployed very close to the IRS such that they only have line-of-sight (LOS) channels to each other, which can be known in advance given their positions. Moreover, define  $\mathbf{g}_{n_h, n_v} = \mathbf{u}_{n_h, n_v} \mathbf{r}_{n_h, n_v}$  as the cascaded channel from the

transmitter to IRS element  $(n_h, n_v)$  to the receiver. At time slot  $t$ , the received signal at the receiver side is then given by

$$\mathbf{y}_t = \mathbf{h}x_t + \sum_{(n_h, n_v) \in \mathcal{E}} e^{j\beta_{n_h, n_v}} \mathbf{g}_{n_h, n_v} x_t + \sum_{(n_h, n_v) \in \mathcal{W}} e^{j\phi_{n_h, n_v, t}} \mathbf{g}_{n_h, n_v} x_t + \mathbf{z}_t, \quad \forall t, \quad (4)$$

where  $x_t$  denotes the known pilot transmitted at time slot  $t$ , and  $\mathbf{z}_t \sim \mathcal{CN}(\mathbf{0}, \sigma^2 \mathbf{I})$  denotes the additive white Gaussian noise (AWGN) of the receiver at time slot  $t$ . Note that the received signals given in (4) are functions of the unknown set  $\mathcal{E}$ . Under the over-the-air approach, we aim to properly design  $\phi_{n_h, n_v, t}$ ,  $\forall n_h, n_v, t$ , such that we can localize all the defective elements in  $\mathcal{E}$  just based on the received signals  $\mathbf{y}_t$ ,  $\forall t$ , without checking the circuit of the IRS.

### III. THREE-PHASE BISECTION METHOD FOR LOCALIZING DEFECTIVE IRS ELEMENTS

The bisection method belongs to the class of the cutting-plane methods, and is widely used to solve the one-dimension optimization problem. In this paper, we will show that the bisection method can also be exploited to localize the defective IRS elements under the over-the-air scheme. For convenience, we will focus on the design of the bisection-based method to estimate  $n_{h, \min}$  and  $n_{h, \max}$  in the horizontal dimension, while the same approach can be utilized to estimate  $n_{v, \min}$  and  $n_{v, \max}$  in the vertical dimension.

The basic idea of our proposed scheme is as follows. Starting with the regime  $[1, N_h]$ , we keep cutting off half of the regime that does not contain  $n_{h, \min}$  ( $n_{h, \max}$ ) until the remaining regime is sufficiently small such that the middle point of this remaining regime can serve as the estimation of  $n_{h, \min}$  ( $n_{h, \max}$ ). In the following, we first show that given any boundary defined by  $c_h = \bar{n}$ , how to determine whether we should cut off the regime on the left hand side of this boundary with  $n_h < \bar{n}$  or the regime on the right hand side of this boundary with  $n_h > \bar{n}$ , just based on the over-the-air measurements. Then, we will introduce our proposed bisection method to iteratively update  $\bar{n}$  and estimate  $n_{h, \min}$  and  $n_{h, \max}$ .

#### A. Determining the Cutting-Plane

Given any boundary defined by  $c_h = \bar{n}$ , our goal is to determine whether  $n_{h, \min}$  ( $n_{h, \max}$ ) is on the left hand side or on the right hand side of this boundary. Depending on the location of the defective IRS elements defined in (1), there are three cases that may occur.

**Case 1:** All the defective IRS elements defined in (1) are on the left hand side of the boundary defined by  $c_h = \bar{n}$ , i.e.,  $n_{h, \min} \leq n_{h, \max} < \bar{n}$ , as shown in Fig. 2 (a).

**Case 2:** All the defective IRS elements defined in (1) are on the right hand side of the boundary defined by  $c_h = \bar{n}$ , i.e.,  $n_{h, \max} \geq n_{h, \min} > \bar{n}$ , as shown in Fig. 2 (b).

**Case 3:** The defective IRS elements defined in (1) are on both the left hand side and the right hand side of the boundary defined by  $c_h = \bar{n}$ , i.e.,  $n_{h, \min} < \bar{n}$  and  $n_{h, \max} > \bar{n}$ , as shown in Fig. 2 (c).

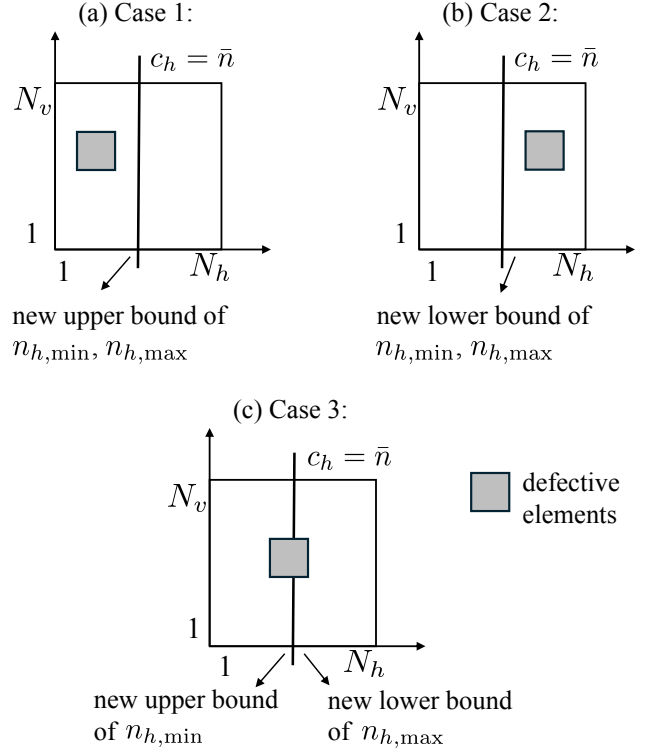


Fig. 2. Three cases of the location of defective elements related to the boundary and the corresponding update of the lower and upper bounds.

In the following, we propose an efficient detection scheme such that given any boundary defined by  $c_h = \bar{n}$ , we can determine which of the above three cases is true.

Under our proposed scheme, there is an initialization stage which consists of two time slots, denoted by time slots  $0_-$  and  $0_+$  for convenience. In time slots  $0_-$  and  $0_+$ , we respectively set a common desired phase shift for all the IRS elements as

$$\phi_{n_h, n_v, 0_-} = \bar{\phi}_{0_-}, \quad \forall n_h, n_v, \quad (5)$$

$$\phi_{n_h, n_v, 0_+} = \bar{\phi}_{0_+} \neq \bar{\phi}_{0_-}, \quad \forall n_h, n_v. \quad (6)$$

Define

$$\mathbf{g}_e = \sum_{(n_h, n_v) \in \mathcal{E}} e^{j\beta_{n_h, n_v}} \mathbf{g}_{n_h, n_v}, \quad (7)$$

$$\mathbf{g}_w = \sum_{(n_h, n_v) \in \mathcal{W}} \mathbf{g}_{n_h, n_v}. \quad (8)$$

According to (4), the received signals in time slots  $0_-$  and  $0_+$  are

$$\mathbf{y}_{0_-} = \mathbf{h}x_{0_-} + \mathbf{g}_e x_{0_-} + \mathbf{g}_w e^{j\bar{\phi}_{0_-}} x_{0_-} + \mathbf{z}_{0_-}, \quad (9)$$

$$\mathbf{y}_{0_+} = \mathbf{h}x_{0_+} + \mathbf{g}_e x_{0_+} + \mathbf{g}_w e^{j\bar{\phi}_{0_+}} x_{0_+} + \mathbf{z}_{0_+}. \quad (10)$$

Because  $\mathbf{z}_{0_-}, \mathbf{z}_{0_+} \sim \mathcal{CN}(\mathbf{0}, \sigma^2 \mathbf{I})$  are independent noise, we have

$$p(\mathbf{y}_{0_-}, \mathbf{y}_{0_+} | \mathbf{g}_e, \mathbf{g}_w) = \frac{1}{(\pi\sigma^2)^{2M}} e^{-\frac{\sum_{i \in \{0_-, 0_+\}} \|\mathbf{y}_i - \mathbf{h}x_i - \mathbf{g}_e x_i - \mathbf{g}_w e^{j\bar{\phi}_i} x_i\|^2}{\sigma^2}}. \quad (11)$$

Then, the maximum-likelihood (ML) estimators of  $\mathbf{g}_e$  and  $\mathbf{g}_w$  that maximize the above conditional probability are given as

$$\bar{\mathbf{g}}_e = \frac{e^{j\bar{\phi}_{0+}}x_{0+}(\mathbf{y}_{0-} - \mathbf{h}x_{0-}) - e^{j\bar{\phi}_{0-}}x_{0-}(\mathbf{y}_{0+} - \mathbf{h}x_{0+})}{x_{0-}x_{0+}(e^{j\bar{\phi}_{0+}} - e^{j\bar{\phi}_{0-}})}, \quad (12)$$

$$\bar{\mathbf{g}}_w = \frac{x_{0-}(\mathbf{y}_{0+} - \mathbf{h}x_{0+}) - x_{0+}(\mathbf{y}_{0-} - \mathbf{h}x_{0-})}{x_{0-}x_{0+}(e^{j\bar{\phi}_{0+}} - e^{j\bar{\phi}_{0-}})}. \quad (13)$$

After the above initialization stage, we make some boundary defined by  $c_h = \bar{n}_t$  at each time slot  $t \geq 1$ , which can divide the whole IRS into two parts. At time slot  $t$ , we respectively set a common desired phase shift for all the IRS elements on the left hand side of the boundary and one for all the IRS elements on the right hand side of the boundary as

$$\phi_{n_h, n_v, t} = \bar{\phi}_{t,l}, \text{ if } n_h \in [1, \lfloor \bar{n}_t \rfloor], \quad (14)$$

$$\phi_{n_h, n_v, t} = \bar{\phi}_{t,r}, \text{ if } n_h \in [\lceil \bar{n}_t \rceil, N_h], \quad t \geq 1, \quad (15)$$

where  $\bar{\phi}_{t,l} \neq \bar{\phi}_{t,r}$ . According to (4) and (7), the received signal at time slot  $t \geq 1$  is

$$\begin{aligned} \mathbf{y}_t = & \mathbf{h}x_t + \mathbf{g}_e x_t + \sum_{(n_h, n_v) \in \mathcal{W}_{t,l}} \mathbf{g}_{n_h, n_v} e^{j\bar{\phi}_{t,l}} x_t + \\ & + \sum_{(n_h, n_v) \in \mathcal{W}_{t,r}} \mathbf{g}_{n_h, n_v} e^{j\bar{\phi}_{t,r}} x_t + \mathbf{z}_t, \quad t \geq 1, \end{aligned} \quad (16)$$

where

$$\mathcal{W}_{t,l} = \{(n_h, n_v) | (n_h, n_v) \in \mathcal{W}, n_h < \bar{n}_t\}, \quad (17)$$

$$\mathcal{W}_{t,r} = \{(n_h, n_v) | (n_h, n_v) \in \mathcal{W}, n_h > \bar{n}_t\}, \quad (18)$$

denote the sets of the normal IRS elements that are on the left hand side and on the right hand side of the boundary defined by  $c_h = \bar{n}_t$ , respectively. Based on the signal received in time slot  $t$  as well as the ML estimators made based on the signals received at time slots  $0_-$  and  $0_+$ , our goal is to detect which of Case 1, Case 2, and Case 3 is true at time slot  $t$ .

Suppose Case 1 is true. This indicates that all the IRS elements on the right hand side of the boundary  $c_h = \bar{n}_t$  are in the normal state, i.e.,  $\mathcal{W}_{t,r} = \{(n_h, n_v) | n_h > \bar{n}_t\}$ . In this case, define

$$\mathbf{g}_{t,r}^{C1} = \sum_{n_h > \bar{n}_t} \sum_{n_v \in \mathcal{N}_v} \mathbf{g}_{n_h, n_v}, \quad (19)$$

$$\mathbf{g}_{t,l}^{C1} = \bar{\mathbf{g}}_w - \mathbf{g}_{t,r}^{C1}, \quad (20)$$

as the estimations of  $\sum_{(n_h, n_v) \in \mathcal{W}_{t,l}} \mathbf{g}_{n_h, n_v}$  and  $\sum_{(n_h, n_v) \in \mathcal{W}_{t,r}} \mathbf{g}_{n_h, n_v}$  in (16) under Case 1. Because  $\mathbf{z}_t \sim \mathcal{CN}(\mathbf{0}, \sigma^2 \mathbf{I})$ , the probability to receive  $\mathbf{y}_t$  at time slot  $t$  given the estimations  $\bar{\mathbf{g}}_e$ ,  $\mathbf{g}_{t,l}^{C1}$ , and  $\mathbf{g}_{t,r}^{C1}$  is

$$\begin{aligned} p(\mathbf{y}_t | \bar{\mathbf{g}}_e, \mathbf{g}_{t,l}^{C1}, \mathbf{g}_{t,r}^{C1}) \\ = \frac{1}{(\pi\sigma^2)^M} e^{-\frac{\|\mathbf{y}_t - \mathbf{h}x_t - \bar{\mathbf{g}}_e x_t - \mathbf{g}_{t,l}^{C1} e^{j\bar{\phi}_{t,l}} x_t - \mathbf{g}_{t,r}^{C1} e^{j\bar{\phi}_{t,r}} x_t\|^2}{\sigma^2}}. \end{aligned} \quad (21)$$

Note that based on the received signals at time slots  $0_-$  and  $0_+$  given in (9) and (10), we estimate  $2M$  variables in  $\mathbf{g}_e$  and  $\mathbf{g}_w$

via  $2M$  equations. Therefore, it is expected that the ML estimators given in (12) and (13) are quite accurate. If Case 1 is true, then  $\mathbf{g}_{t,r}^{C1}$  and  $\mathbf{g}_{t,l}^{C1}$  given in (19) and (20) are also very accurate estimators of  $\sum_{(n_h, n_v) \in \mathcal{W}_{t,r}} \mathbf{g}_{n_h, n_v}$  and  $\sum_{(n_h, n_v) \in \mathcal{W}_{t,l}} \mathbf{g}_{n_h, n_v}$ . To summarize, the conditional probability given in (21) will be quite high if Case 1 is true. Otherwise, if Case 1 is not true, then  $\mathbf{g}_{t,r}^{C1}$  and  $\mathbf{g}_{t,l}^{C1}$  given in (19) and (20) are poor estimators. Therefore, a very large noise power of  $\mathbf{z}_t$  can make the equation in (16) hold given the above poor estimators. To summarize, the conditional probability given in (21) will be quite low if Case 1 is not true. Consequently, we claim that Case 1 is true if and only if

$$p(\mathbf{y}_t | \bar{\mathbf{g}}_e, \mathbf{g}_{t,l}^{C1}, \mathbf{g}_{t,r}^{C1}) > \bar{p}_1, \quad (22)$$

where  $\bar{p}_1$  is a pre-determined threshold.

Next, if Case 2 is true, all the IRS elements on the left hand side of the boundary  $c_h = \bar{n}_t$  are in the normal state, i.e.,  $\mathcal{W}_{t,l} = \{(n_h, n_v) | n_h < \bar{n}_t\}$ . Define

$$\mathbf{g}_{t,l}^{C2} = \sum_{n_h < \bar{n}_t} \sum_{n_v \in \mathcal{N}_v} \mathbf{g}_{n_h, n_v}, \quad (23)$$

$$\mathbf{g}_{t,r}^{C2} = \bar{\mathbf{g}}_w - \mathbf{g}_{t,l}^{C2}, \quad (24)$$

as the estimations of  $\sum_{(n_h, n_v) \in \mathcal{W}_{t,l}} \mathbf{g}_{n_h, n_v}$  and  $\sum_{(n_h, n_v) \in \mathcal{W}_{t,r}} \mathbf{g}_{n_h, n_v}$  in (16) under Case 2. Similar to (21), the probability to receive  $\mathbf{y}_t$  at time slot  $t$  given the estimations  $\bar{\mathbf{g}}_e$ ,  $\mathbf{g}_{t,l}^{C2}$ , and  $\mathbf{g}_{t,r}^{C2}$  is

$$\begin{aligned} p(\mathbf{y}_t | \bar{\mathbf{g}}_e, \mathbf{g}_{t,l}^{C2}, \mathbf{g}_{t,r}^{C2}) \\ = \frac{1}{(\pi\sigma^2)^M} e^{-\frac{\|\mathbf{y}_t - \mathbf{h}x_t - \bar{\mathbf{g}}_e x_t - \mathbf{g}_{t,l}^{C2} e^{j\bar{\phi}_{t,l}} x_t - \mathbf{g}_{t,r}^{C2} e^{j\bar{\phi}_{t,r}} x_t\|^2}{\sigma^2}}. \end{aligned} \quad (25)$$

We claim that Case 2 is true if and only if

$$p(\mathbf{y}_t | \bar{\mathbf{g}}_e, \mathbf{g}_{t,l}^{C2}, \mathbf{g}_{t,r}^{C2}) > \bar{p}_2, \quad (26)$$

where  $\bar{p}_2$  is a pre-determined threshold.

At last, we claim that Case 3 is true if and only if both (22) and (26) do not hold,<sup>2</sup> i.e.,

$$p(\mathbf{y}_t | \bar{\mathbf{g}}_e, \mathbf{g}_{t,l}^{C1}, \mathbf{g}_{t,r}^{C1}) \leq \bar{p}_1, \quad (27)$$

$$p(\mathbf{y}_t | \bar{\mathbf{g}}_e, \mathbf{g}_{t,l}^{C2}, \mathbf{g}_{t,r}^{C2}) \leq \bar{p}_2. \quad (28)$$

### B. Three-Phase Bisection Method

After introducing how to make the cutting plane, in the following, we propose a novel three-phase bisection method to estimate  $n_{h,\min}$  and  $n_{h,\max}$  in the horizontal dimension, based on the over-the-air measurements.

Specifically, define  $n_{h,\min}^{\text{lb},0} = 1$  ( $n_{h,\max}^{\text{lb},0} = 1$ ) and  $n_{h,\min}^{\text{ub},0} = N_h$  ( $n_{h,\max}^{\text{ub},0} = N_h$ ) as the initial lower bound and upper bound of  $n_{h,\min}$  ( $n_{h,\max}$ ). In time slots  $0_-$  and  $0_+$ , we set desired IRS phase shifts according to (5) and (6), keep a record of the received signals shown in (9) and (10), and make ML

<sup>2</sup>If both (22) and (26) hold, it indicates that all the IRS elements are detected to be in the normal state, i.e., a diagnosis of the IRS is no longer needed. Because this paper assumes that there exist defective elements on the IRS, the above case is very unlikely to occur if  $\bar{p}_1$  and  $\bar{p}_2$  are properly selected.

estimations of  $\mathbf{g}_e$  and  $\mathbf{g}_w$  based on (12) and (13). After the above initialization stage, we conduct the  $t$ -th iteration of the bisection method based on the signal received at time slot  $t$  via applying the detection method proposed in the previous subsection. Let  $n_{h,\min}^{\text{lb},t}$  ( $n_{h,\max}^{\text{lb},t}$ ) and  $n_{h,\min}^{\text{ub},t}$  ( $n_{h,\max}^{\text{ub},t}$ ) denote the lower bound and the upper bound of  $n_{h,\min}$  ( $n_{h,\max}$ ) obtained after the  $t$ -th iteration of our bisection method. Depending on which bounds are updated, we divide the whole process of our proposed bisection method into three phases.

1) *Phase I*: Phase I is the phase where the bounds of  $n_{h,\min}$  and  $n_{h,\max}$  are updated together at one iteration. Specifically, in the first a few iterations of the bisection method,  $n_{h,\min}$  and  $n_{h,\max}$  have the same lower bound and the same upper bound. For example, at the initialization stage, we have  $n_{h,\min}^{\text{lb},0} = n_{h,\max}^{\text{lb},0} = 1$  and  $n_{h,\min}^{\text{ub},0} = n_{h,\max}^{\text{ub},0} = N_h$ . If  $n_{h,\min}^{\text{lb},t} = n_{h,\max}^{\text{lb},t}$  and  $n_{h,\min}^{\text{ub},t} = n_{h,\max}^{\text{ub},t}$  are true at the  $t$ -th iteration, then at the  $(t+1)$ -th iteration, the boundary for estimating  $n_{h,\min}$ , which is defined by the middle point of the regime  $[n_{h,\min}^{\text{lb},t}, n_{h,\min}^{\text{ub},t}]$ , i.e.,  $n_{h,\min}^{\text{md},t+1} = (n_{h,\min}^{\text{lb},t} + n_{h,\min}^{\text{ub},t})/2$ , and the boundary for estimating  $n_{h,\max}$ , which is defined by the middle point of the regime  $[n_{h,\max}^{\text{lb},t}, n_{h,\max}^{\text{ub},t}]$ , i.e.,  $n_{h,\max}^{\text{md},t+1} = (n_{h,\max}^{\text{lb},t} + n_{h,\max}^{\text{ub},t})/2$ , are the same, i.e.,  $n_{h,\min}^{\text{md},t+1} = n_{h,\max}^{\text{md},t+1}$ . Therefore, we can simultaneously update the bounds of  $n_{h,\min}$  and  $n_{h,\max}$  at the  $(t+1)$ -th iteration as follows. At time slot  $t+1$ , we set the boundary as  $c_h = \bar{n}_{t+1} = n_{h,\min}^{\text{md},t+1} = n_{h,\max}^{\text{md},t+1}$  and the phase shifts of IRS elements based on (14) and (15). Based on the signal received at time slot  $t+1$ , i.e.,  $\mathbf{y}_{t+1}$ , if Case 1 is true, i.e., (22) holds, then we update the new bounds as  $n_{h,\min}^{\text{lb},t+1} = n_{h,\max}^{\text{lb},t+1} = n_{h,\min}^{\text{lb},t}$  and  $n_{h,\min}^{\text{ub},t+1} = n_{h,\max}^{\text{ub},t+1} = \lfloor n_{h,\min}^{\text{md},t+1} \rfloor$ . If Case 2 is true, i.e., (26) holds, then we update the new bounds as  $n_{h,\min}^{\text{lb},t+1} = n_{h,\max}^{\text{lb},t+1} = \lceil n_{h,\min}^{\text{md},t+1} \rceil$  and  $n_{h,\min}^{\text{ub},t+1} = n_{h,\max}^{\text{ub},t+1} = n_{h,\min}^{\text{ub},t}$ . If Case 3 is true, i.e., both (27) and (28) hold, then we update the new bounds as  $n_{h,\min}^{\text{lb},t+1} = n_{h,\min}^{\text{lb},t}$ ,  $n_{h,\min}^{\text{ub},t+1} = \lfloor n_{h,\min}^{\text{md},t+1} \rfloor$ ,  $n_{h,\max}^{\text{lb},t+1} = \lceil n_{h,\max}^{\text{md},t+1} \rceil$ , and  $n_{h,\max}^{\text{ub},t+1} = n_{h,\max}^{\text{ub},t}$ .

Note that if Case 1 or Case 2 is true, we still have  $n_{h,\min}^{\text{lb},t+1} = n_{h,\max}^{\text{lb},t+1}$  and  $n_{h,\min}^{\text{ub},t+1} = n_{h,\max}^{\text{ub},t+1}$  at the  $(t+1)$ -th iteration. Otherwise, if Case 3 is true, we have  $n_{h,\min}^{\text{lb},t+1} \neq n_{h,\max}^{\text{lb},t+1}$  and  $n_{h,\min}^{\text{ub},t+1} \neq n_{h,\max}^{\text{ub},t+1}$  at the  $(t+1)$ -th iteration. Define  $t^I$  as the index of the iteration where Case 3 occurs for the first time. Then, Phase I of our proposed bisection method ends at the  $t^I$ -th iteration, when the boundary passes through the cluster of defective IRS elements for the first time such that the bounds of  $n_{h,\min}$  and  $n_{h,\max}$  are different.

One example about the update of the bounds in three cases of Phase I can be found in Fig. 2.

2) *Phase II*: Phase II starts at time slot  $t^I+1$  and is the phase where merely the bounds of  $n_{h,\min}$  are updated until  $n_{h,\min}$  is found. At iteration  $t+1$  with  $t \geq t^I$ , the new boundary is  $c_h = n_{h,\min}^{\text{md},t+1} = (n_{h,\min}^{\text{lb},t} + n_{h,\min}^{\text{ub},t})/2$ . Based on the signal received at time slot  $t+1$ , if Case 2 is true, we set  $n_{h,\min}^{\text{lb},t+1} = \lceil n_{h,\min}^{\text{md},t+1} \rceil$  and  $n_{h,\min}^{\text{ub},t+1} = n_{h,\min}^{\text{ub},t}$ . If Case 3 is true, we set  $n_{h,\min}^{\text{lb},t+1} = n_{h,\min}^{\text{lb},t}$  and  $n_{h,\min}^{\text{ub},t+1} = \lfloor n_{h,\min}^{\text{md},t+1} \rfloor$ . Define  $t^{\text{II}}$  as the

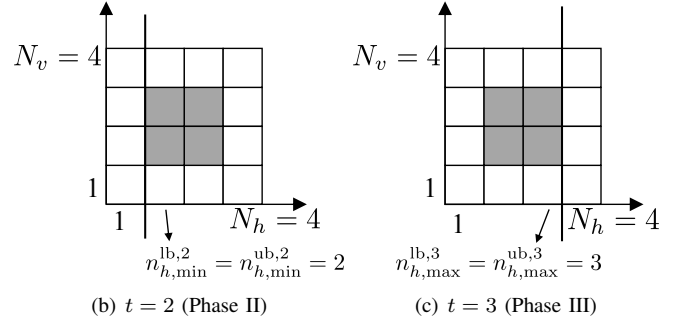
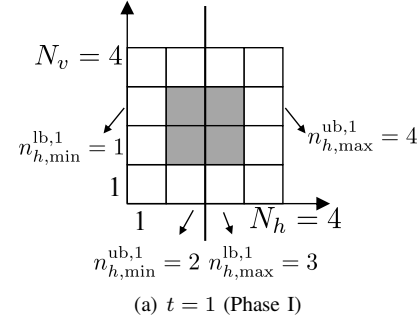


Fig. 3. An illustration of our proposed three-phase bisection approach for localizing defective IRS elements.

index of the iteration where  $n_{h,\min}^{\text{lb},t^{\text{II}}} = n_{h,\min}^{\text{ub},t^{\text{II}}}$ . Then, Phase II ends at the  $t^{\text{II}}$ -th iteration, and  $n_{h,\min}$  is estimated as  $n_{h,\min}^{\text{lb},t^{\text{II}}}$ .

3) *Phase III*: Phase III starts at time slot  $t^{\text{II}}+1$  and is the phase where merely the bounds of  $n_{h,\max}$  are updated until  $n_{h,\max}$  is found. At iteration  $t+1$  with  $t \geq t^{\text{II}}$ , the new boundary is  $c_h = n_{h,\max}^{\text{md},t+1} = (n_{h,\max}^{\text{lb},t} + n_{h,\max}^{\text{ub},t})/2$ . Based on the signal received at time slot  $t+1$ , if Case 1 is true, we set  $n_{h,\max}^{\text{ub},t+1} = \lfloor n_{h,\max}^{\text{md},t+1} \rfloor$  and  $n_{h,\max}^{\text{lb},t+1} = n_{h,\max}^{\text{lb},t}$ . If Case 3 is true, we set  $n_{h,\max}^{\text{lb},t+1} = \lceil n_{h,\max}^{\text{md},t+1} \rceil$  and  $n_{h,\max}^{\text{ub},t+1} = n_{h,\max}^{\text{ub},t}$ . Define  $t^{\text{III}}$  as the index of the iteration where  $n_{h,\max}^{\text{lb},t^{\text{III}}} = n_{h,\max}^{\text{ub},t^{\text{III}}}$ . Then, Phase III ends at the  $t^{\text{III}}$ -th iteration, and  $n_{h,\max}$  is estimated as  $n_{h,\max}^{\text{lb},t^{\text{III}}}$ .

*Example 1*: In the following, we provide an example to illustrate how the above three-phase bisection approach works to iteratively find  $n_{h,\min}$  and  $n_{h,\max}$  in the horizontal domain. In this example, we assume that on an IRS consisting of  $4 \times 4$  elements, all the defective IRS elements are located at the regime  $\mathcal{E} = \{(n_h, n_v) | n_h \in \{2, 3\}, n_v \in \{2, 3\}\}$ , as shown in Fig. 3. Specifically, at the initial stage, we have  $n_{h,\min}^{\text{lb},0} = n_{h,\max}^{\text{lb},0} = 1$  and  $n_{h,\min}^{\text{ub},0} = n_{h,\max}^{\text{ub},0} = N_h = 4$ . As shown in Fig. 3(a), at the first time slot, which is Phase I, the boundary to cut in the horizontal domain is  $c_h = 2.5$ , which is useful for updating the bounds for both  $n_{h,\min}$  and  $n_{h,\max}$ . Based on the detectors shown in (22)-(28), Case 3 should be detected. In this case, we update  $n_{h,\min}^{\text{ub},1} = 2$ ,  $n_{h,\max}^{\text{lb},1} = 3$ , and keep  $n_{h,\min}^{\text{lb},1} = n_{h,\min}^{\text{lb},0} = 1$  and  $n_{h,\max}^{\text{ub},1} = n_{h,\max}^{\text{ub},0} = 4$ . Because Case 3 has occurred, Phase I ends after the first iteration. As shown in Fig. 3(b), at the second time slot, which is Phase II, the boundary to cut in the horizontal domain is  $c_h = 1.5$ , which is useful for checking whether  $n_{h,\min} > 1.5$  or  $n_{h,\min} < 1.5$ . Based on the detectors shown in (22)-(28), Case 2 should

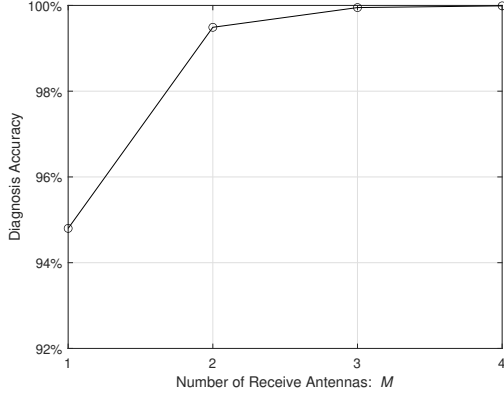


Fig. 4. Performance of our method for localizing defective IRS elements.

be detected. In this case, we update  $n_{h,\min}^{\text{lb},2} = 2$ , and keep  $n_{h,\min}^{\text{ub},2} = n_{h,\min}^{\text{ub},1} = 2$ . Because  $n_{h,\min}^{\text{lb},2} = n_{h,\min}^{\text{ub},2} = 2$ , Phase II ends and  $n_{h,\min} = 2$  can be determined. As shown in Fig. 3(c), at the third time slot, which is Phase III, the boundary to cut in the horizontal domain is  $c_h = 3.5$ , which is useful for updating the bounds for  $n_{h,\max}$ . Similarly, based on the detectors shown in (22)-(28), Case 1 should be detected. In this case, we update  $n_{h,\max}^{\text{ub},3} = 3$ , and keep  $n_{h,\max}^{\text{lb},3} = n_{h,\max}^{\text{lb},1} = 3$ . Because  $n_{h,\max}^{\text{lb},3} = n_{h,\max}^{\text{ub},3} = 3$ , Phase III ends and  $n_{h,\max} = 3$  can be determined. After three iterations, the values of  $n_{h,\min}$  and  $n_{h,\max}$  are known. We can also apply the above approach to estimate  $n_{v,\min}$  and  $n_{v,\max}$  in the vertical domain.

#### IV. NUMERICAL RESULTS

In this section, we provide a numerical example to verify the effectiveness of the proposed method for localizing the defective IRS elements based on over-the-air measurements. We assume that there are  $N = 1024$  elements on an IRS, with  $N_h = N_v = 32$ . Moreover, we assume that the transmitter, the receiver, and the IRS are deployed in the near-field regime of each other. Therefore,  $\mathbf{h}$ ,  $\mathbf{r}_{n_h, n_v}$ , and  $u_{n_h, n_v}$  are generated based on the near-field LOS channel model [19]. In each realization, we randomly generate the locations of the transmitter, the receiver, the IRS, and the defective elements on the IRS. We claim that the diagnosis is accurate in one realization only when  $n_{h,\min}$ ,  $n_{h,\max}$ ,  $n_{v,\min}$ , and  $n_{v,\max}$  are all correctly estimated. Fig. 4 shows the performance of our proposed scheme. It is observed that the diagnosis accuracy is around 95% when  $M = 1$ , and very close to 100% when  $M \geq 3$ . This is because with more receive antennas, we have more observations to localize the defective elements. This numerical example (together with many other examples that are not shown here due to space limitation) verifies the possibility to perform over-the-air diagnosis of the IRS.

#### V. CONCLUSION

In this paper, we investigated the possibility to find the defective IRS elements based on the over-the-air measurements. To achieve this goal, we designed a novel three-phase bisection method, under which we can iteratively remove half of the

interested regime that does not contain the boundary of the defective IRS elements. Our results provided a new approach to perform diagnosis of the IRS.

#### REFERENCES

- [1] C. Liaskos, S. Nie, A. Tsioliaridou, A. Pitsillides, S. Ioannidis, and I. Akyildiz, "A new wireless communication paradigm through software-controlled metasurfaces," *IEEE Commun. Mag.*, vol. 56, no. 9, pp. 162–169, Sep. 2018.
- [2] M. D. Renzo *et al.*, "Smart radio environments empowered by reconfigurable AI meta-surfaces: An idea whose time has come," *EURASIP J. Wireless Commun. Network.*, no. 129, pp. 1–20, May 2019.
- [3] E. Basar, M. D. Renzo, J. Rosny, M. Debbah, M.-S. Alouini, and R. Zhang, "Wireless communications through reconfigurable intelligent surfaces," *IEEE Access*, vol. 7, pp. 116 753–116 773, 2019.
- [4] Q. Wu, S. Zhang, B. Zheng, C. You, and R. Zhang, "Intelligent reflecting surface-aided wireless communications: A tutorial," *IEEE Trans. Commun.*, vol. 69, no. 5, pp. 3313–3351, May 2021.
- [5] Z. Wang, L. Liu, and S. Cui, "Channel estimation for intelligent reflecting surface assisted multiuser communications: Framework, algorithms, and analysis," *IEEE Trans. Wireless Commun.*, vol. 19, no. 10, pp. 6607–6620, Oct. 2020.
- [6] H. Liu, X. Yuan, and Y.-J. A. Zhang, "Matrix-calibration-based cascaded channel estimation for reconfigurable intelligent surface assisted multiuser MIMO," *IEEE J. Sel. Areas Commun.*, vol. 38, no. 11, pp. 2621–2636, Jul. 2020.
- [7] G. Zhou, C. Pan, H. Ren, P. Popovski, and A. L. Swindlehurst, "Channel estimation for RIS-aided multiuser millimeter-wave systems," *IEEE Trans. Signal Process.*, vol. 70, pp. 1478–1492, 2022.
- [8] J. Chen, Y.-C. Liang, H. V. Cheng, and W. Yu, "Channel estimation for reconfigurable intelligent surface aided multi-user MIMO systems," *IEEE Trans. Wireless Commun.*, vol. 22, no. 10, pp. 6853–6869, Oct. 2023.
- [9] S. Zhang and R. Zhang, "Capacity characterization for intelligent reflecting surface aided MIMO communication," *IEEE J. Sel. Areas Commun.*, vol. 38, no. 8, pp. 1823–1838, Jun. 2020.
- [10] Q. Wu and R. Zhang, "Intelligent reflecting surface enhanced wireless network: joint active and passive beamforming design," in *Proc. IEEE Global Commun. Conf. (GLOBECOM)*, Dec. 2018.
- [11] C. Huang, A. Zappone, G. C. Alexandropoulos, M. Debbah, and C. Yuen, "Reconfigurable intelligent surfaces for energy efficiency in wireless communication," *IEEE Trans. Wireless Commun.*, vol. 18, no. 8, pp. 4157–4170, Aug. 2019.
- [12] H. Guo, Y.-C. Liang, J. Chen, and E. G. Larsson, "Weighted sum-rate maximization for reconfigurable intelligent surface aided wireless networks," *IEEE Trans. Wireless Commun.*, vol. 19, no. 5, pp. 3064–3076, May 2020.
- [13] X. Yu, D. Xu, Y. Sun, D. W. K. Ng, and R. Schober, "Robust and secure wireless communications via intelligent reflecting surfaces," *IEEE J. Sel. Areas Commun.*, vol. 38, no. 11, pp. 2637–2652, Nov. 2020.
- [14] H. Taghvaei, A. Cabellos-Aparicio, J. Georgiou, and S. Abadal, "Error analysis of programmable metasurfaces for beam steering," *IEEE J. Emerg. Sel. Top. Circuits Syst.*, vol. 10, no. 1, pp. 62–74, Mar. 2020.
- [15] M. Badiu and J. P. Coon, "Communication through a large reflecting surface with phase errors," *IEEE Wireless Commun. Lett.*, vol. 9, no. 2, pp. 184–188, Feb. 2020.
- [16] A. M. T. Khel and K. A. Hamdi, "Effects of hardware impairments on IRS-enabled MISO wireless communication systems," *IEEE Commun. Lett.*, vol. 26, no. 2, pp. 259–263, Feb. 2022.
- [17] X. Qian, M. D. Renzo, J. Liu, A. Kammoun, and M.-S. Alouini, "Beamforming through reconfigurable intelligent surfaces in single-user MIMO systems: SNR distribution and scaling laws in the presence of channel fading and phase noise," *IEEE Wireless Commun. Lett.*, vol. 10, no. 1, pp. 77–81, Jan. 2021.
- [18] J. Zhang, X. Hu, and C. Zhong, "Phase calibration for intelligent reflecting surfaces assisted millimeter wave communications," *IEEE Trans. Signal Process.*, vol. 70, pp. 1026–1040, 2022.
- [19] D. Tse and P. Viswanath, *Fundamentals of Wireless Communication*. Cambridge, UK: Cambridge University Press, 2005.